Elevated expression of endogenous glial cell line-derived neurotrophic factor impairs spatial memory performance and raises inhibitory tone in the hippocampus

Pepin Marshall, Daniel R Garton, Tomi Taira, Vootele Võikar, Carolina Vilenius, Natalia Kulesskaya, Claudio Rivera, Jaan-olle Andressoo

Received: 29 April 2020 | Revised: 7 January 2021 | Accepted: 19 January 2021

DOI: 10.1111/ejn.15126

RESEARCH REPORT

EJN European Journal of Neuroscience FENS WILEY

Elevated expression of endogenous glial cell line-derived neurotrophic factor impairs spatial memory performance and raises inhibitory tone in the hippocampus

Pepin Marshall[1] | **Daniel R. Garton**[4] | **Tomi Taira**[1,2] | **Vootele Võikar**[1] | **Carolina Vilenius**[1] | **Natalia Kulesskaya**[1] | **Claudio Rivera**[1,3] | **Jaan-Olle Andressoo**[4,5]

[1]HiLIFE Neuroscience Centre, University of Helsinki, Helsinki, Finland

[2]Veterinary Biosciences, University of Helsinki, Helsinki, Finland

[3]Institut de Neurobiologie de la Méditerranée, INMED UMR901, Marseille, France

[4]Department of Pharmacology, Faculty of Medicine & Helsinki Institute of Life Science (HiLIFE) Helsinki, University of Helsinki, Helsinki, Finland

[5]Karolinska Institute, Division of Neurogeriatrics, Department of Neurobiology, Care Sciences and Society (NVS), Stockholm, Sweden

Correspondence
Jaan-Olle Andressoo, University of Helsinki, Department of Pharmacology, Faculty of Medicine & Helsinki Institute of Life Science (HiLIFE) Helsinki, Finland.
Email: jaan-olle.andressoo@helsinki.fi

Funding information
Instrumentarium Foundation; Academy of Finland, Grant/Award Number: 1308265, 266820 and 297727; Sigrid Juselius Foundation; University of Helsinki; Helsinki Institute of Life Science; European Research Council, Grant/Award Number: 724922; Alzheimerfonden; Jane and Aatos Erkko Foundation; Biocenter Finland

Abstract

Parvalbumin-positive interneurons (PV+) are a key component of inhibitory networks in the brain and are known to modulate memory and learning by shaping network activity. The mechanisms of PV+ neuron generation and maintenance are not fully understood, yet current evidence suggests that signalling via the glial cell line-derived neurotrophic factor (GDNF) receptor GFRα1 positively modulates the migration and differentiation of PV+ interneurons in the cortex. Whether GDNF also regulates PV+ cells in the hippocampus is currently unknown. In this study, we utilized a *Gdnf* "hypermorph" mouse model where GDNF is overexpressed from the native gene locus, providing greatly increased spatial and temporal specificity of protein expression over established models of ectopic expression. $Gdnf^{wt/hyper}$ mice demonstrated impairments in long-term memory performance in the Morris water maze test and an increase in inhibitory tone in the hippocampus measured

Abbreviations: ANOVA, analysis of variance; ATP, adenosine triphosphate; BSA, bovine serum albumin; CA1, cornu ammonis 1; CA3, cornu ammonis 3; CTX, cortex; D1, dopamine receptor 1; D5, dopamine receptor 5; DA, dopamine; DAergic, dopaminergic; DAT, dopamine transporter; DG, dentate gyrus; DMSO, dimethylsulfoxide; DOPAC, 3,4-dihydroxyphenylacetic acid; EGTA, ethylene glycol-bis(β-aminoethyl ether)-N,N,N′,N′-tetraacetic acid; GABAA, GABA receptor type A; GABA, γ-aminobutyric acid; GDNF, glial cell line-derived neurotrophic factor; $Gdnf^{wt/hyper}$, Gdnf wild-type / hypermorphic heterozygote; $Gdnf^{wt/wt}$, Gdnf wild-type / wild-type; GFRα1, GDNF family receptor alpha 1; GFRα2, GDNF family receptor alpha 2; GTP, guanosine triphosphate; HEPES, 4-(2-hydroxyethyl)-1-piperazineethanesulfonic acid; IBM, International Business Machines; IT, initial training; mIPSC, minitature inhibitory post-synaptic current; mV, millivolt; N-syndecan, 3N-terminal syndecan 3; pA, picoampere; PBS, phosphate-buffered saline; PP, posteriorparietal cortex; PT, probe trials; PTZ, pentylenetetrazole; PV+, parvalbumin-positive; PV, parvalbumin; RET, rearranged during transfection; RSP, retrosplenial cortex; RT, reversal training; S1B, primary somatosensory cortex, barrer; S1T, primary somatosensory cortex, trunk; SD, standard deviation; SEM, standard error of the mean; sIPSC, spontaneous inhibitory post-synaptic current; SPSS, Statistics Package for Social Scientists; SS, somatosensory cortex; TBSTD, tris buffered saline with 0.1% tween and 5% DMSO; WM, water maze; WRJ, wild running and jumping.

Edited by: Marco Capogna

electrophysiologically in acute brain slice preparations. Increased PV+ cell number was confirmed immunohistochemically in the hippocampus and in discrete cortical areas and an increase in epileptic seizure threshold was observed in vivo. The data consolidate prior evidence for the actions of GDNF as a regulator of PV+ cell development in the cortex and demonstrate functional effects upon network excitability via modulation of functional GABAergic signalling and under epileptic challenge.

KEYWORDS

epilepsy, GABA, mouse models, pentylenetetrazole

1 | INTRODUCTION

Parvalbumin-expressing interneurons (PV+) comprise around 40% of all interneurons in the brain (Markram et al., 2004) and are critical modulators of brain activity (Cobb et al., 1995; Fukuda & Kosaka, 2000a, 2000b; Kawaguchi et al., 1987). Altered PV+ interneuron function and expression is associated with neuropsychiatric conditions (Marín, 2012) and GABAergic function more broadly with epilepsy (Galanopoulou, 2010; Olsen & Avoli, 1997). PV+ interneurons have also recently been shown to co-ordinate the network dynamics of episodic memory consolidation in vivo (Donato et al., 2013; Ognjanovski et al., 2017). Understanding the development and function of interneurons is therefore important for understanding brain function and human diseases.

Glial cell line-derived neurotrophic factor (GDNF (Lin et al., 1993)) has broad effects in the development of multiple cell types in the periphery and central nervous system (see Ibáñez & Andressoo, 2015 for review). GDNF acts by binding to its primary receptor, GDNF family receptor alpha-1 (GFRα1) and signalling via the RET tyrosine kinase receptor (Durbec et al., 1996; Jing et al., 1996; Treanor et al., 1996; Trupp et al., 1996). Whilst GFRα1 is broadly expressed in the central nervous system, RET expression is restricted and GDNF then signals independently of RET via neural cell adhesion molecule (NCAM; Paratcha et al., 2003), or N-Syndecan-3 (Bespalov et al., 2011). Illustrating this, only GDNF or GFRα1 knockout mice show reduced numbers of cortical and hippocampal interneurons at birth, yet RET knockout animals do not (Pozas & Ibáñez, 2005). However, one challenge that has hampered advances in studying the postnatal role of GDNF signalling is the early postnatal lethality of GDNF knockout mice due to lack of kidneys and enteric nerves (Moore et al., 1996; Pichel et al., 1996; Sánchez et al., 1996).

To overcome the problem posed by early postnatal lethality and gain insight into how GDNF signalling impacts the postnatal brain, transgenic mice were generated where GFRα1 expression is limited solely to RET expressing cells; "cis-only" (Canty et al., 2009). These animals survive the postnatal period as they develop kidneys and enteric nerves and develop grossly normally (Enomoto et al., 1998). Interestingly, about 72% of parvalbumin positive (PV+) interneurons do not express RET in the hippocampus, yet the majority of PV+ interneurons are positive for GFRα1 (Sarabi et al., 2000), suggesting a role for GDNF in PV+ cell development and function, independent of signalling via RET. In line with this hypothesis, Canty et al. (2009) described disruption in the location of cortical PV+ interneurons in medial and rostrocaudal regions and concomitant cortical hyperexcitability in GFRα1 "cis-only" mice. These results suggest that RET-independent GDNF signalling is important in regulating PV+ development and function in the cortex. Furthermore, mice lacking GDNF family ligand neurturin (NRTN) binding receptor GFRα2 show memory impairment, further supporting the idea that RET-independent signalling regulates cortial and hippocampal development (Võikar et al., 2004). Finally, GDNF is induced by epileptiform activity and ectopic GDNF application is anti-epileptogenic when applied directly into the brain – most of which does not express RET (Humpel et al., 1994; Kanter-Schlifke et al., 2009; Martin et al., 1995; Mikuni et al., 1999; Reeben et al., 1998; Schmidt-Kastner et al., 1994; Yoo et al., 2006). Yet how endogenous GDNF regulates neuronal excitability, memory, and PV+ cell development and adult function in the physiological situation when the GFRα1 receptor is expressed in natively-expressing cells and not restricted to RET-expressing cells is currently unknown.

Previously, we reported generation of a mouse model where GDNF expression from its native locus is increased about twofold in heterozygous mutants. This is achieved by replacing the *Gdnf* 3'UTR with a one which promotes *Gdnf* mRNA stability (Kumar et al., 2015). Because the 3'UTR affects expression post-transcriptionally, this approach results in an increase in expression limited solely to those cells that normally transcribe *Gdnf*. We found that $Gdnf^{wt/hyper}$ mice display enhanced GDNF signalling and – apart from improved motor function - do not display any of the behavioural or molecular side effects associated with ectopic GDNF expression in the brain (Kumar et al., 2015; Mätlik et al., 2018). Because $Gdnf^{wt/hyper}$ mice are viable they present an opportunity to study the effect of endogenous GDNF on brain postnatal development

and function. Here, we present the finding that long-term memory performance in the Morris water maze test in *Gdnf*$^{wt/hyper}$ mice is impaired. This is paralleled by an increase in PV+ interneurons in the dorsal hippocampus and in distinct cortical areas. We observe an increase in inhibitory tone in acute hippocampal slice preparations in vitro which parallels with an increase in seizure threshold in vivo. These results suggest that GDNF levels regulate cortical and hippocampal PV+ neuron development and regulate inhibitory function in vivo.

2 | MATERIALS AND METHODS

2.1 | GDNF hypermorphic mice

The production of *Gdnf* hypermorph heterozygous mice (*Gdnf*$^{wt/hyper}$) was performed as described by Kumar et al. (2015). Briefly, *Gdnf 3'UTR* replacement was performed via insertion of an FRT-flanked puΔtk cassette (Chen & Bradley, 2000) after the stop codon in the *Gdnf* locus in embryonic stem (ES) cells. The puΔtk cassette contains the bovine growth hormone polyadenylation (bGHpA) signal which terminates transcription. In silico analysis demonstrated that puΔtk contains approximately half the number of potential miRNA-binding sites and ~10% of the conserved miRNA sites present in the wild-type *Gdnf* 3'UTR, resulting in a lack of sites for miRNA-induced down-regulation of *Gdnf* and a subsequent increase in gene expression (Kumar et al., 2015).

Gdnf "hypermorph" mice were maintained in a 129Ola/ICR/C57bl6 mixed background. *Gdnf*$^{wt/hyper}$ males (heterozygotes) were bred with wild-type females to produce offspring with a Mendelian distribution of ~50% wild-type and 50% heterozygous *Gdnf*$^{wt/hype}$ littermate animals were used as controls. For the electrophysiology experiments *Gdnf*$^{wt/hyper}$ males were bred with wild-type C57Bl/6JRccHSd (Envigo). All animal experiments were performed in accordance with the Council Directive 2010/63EU of the European Parliament and the Council of 22 September 2010 on the protection of animals used for scientific purposes. The number of animals was kept to a minimum and they were treated in a humane manner in compliance with the guidelines of the Helsinki University Animal Care Committee and approved by the County Administrative Board of Southern Finland under licence numbers ESAVI-2010-09011/Ym-23 and ESAVI/11198/04.10.07/2014.

2.2 | Morris water maze

44 male mice (22 *Gdnf*$^{wt/hyper}$ and 22 *Gdnf*$^{wt/wt}$ wild-type littermate controls) were tested. The mice were group-housed (2–4 animals per cage) with food and water ad libitum under a 12-hr light-dark cycle (lights on at 6 a.m.) at relative humidity 50%–60% and room temperature 21 ± 1°C. The bedding (aspen chips, Tapvei Oy, Finland) was changed weekly and a wooden tube and aspen shavings (Tapvei) was provided as an enrichment. The age of the mice at the beginning of behavioural testing was 3 months. There was no difference in the body weight of the animals in the beginning of testing (*Gdnf*$^{wt/wt}$ 35.7 ± 0.6 g, *Gdnf*$^{wt/hyper}$ 34.7 ± 0.5 g).

The system consisted of a black circular swimming pool (Ø 120 cm) and an escape platform (Ø 10 cm) submerged 0.5 cm under the water surface in the centre of one of four imaginary quadrants. Noldus Ethovision XT 10 software (Noldus Information Technology) was used for tracking and recording the trials in water maze. The animals were released to swim in random positions facing the wall and the time to reach the escape platform (maximum time 60 s) and the swimming distance were measured in every session. In addition, thigmotaxis (time spent swimming within the outermost ring of the pool 10 cm from the wall) was measured. Two training sessions consisting of three trials each were conducted daily. The interval between trials was 4–5 min and between training sessions ~5 hr. The hidden platform remained in a constant location for 3 days (for the six initial training sessions) and was thereafter moved to the opposite quadrant for 2 days (four reversal training sessions). The probe trials (PT) were conducted approximately 18 hr after the last initial training session and the last reversal training session. For probe trials mice swam in the maze for 60 s without the platform being available. Spatial memory in the probe trials is therefore estimated by preference for swimming within the trained quadrant (a circular area of Ø 30 cm surrounding the previously trained platform location) over swimming in corresponding regions in the three other quadrants. After the second probe trial, mice were tested as a control for one block of three trials with the platform made fully visible in a quadrant not previously used to see if escape latency was affected (VIS). Statistical analyses were performed in SPSS (IBM Corp. Released 2016. IBM SPSS Statistics for Windows, Version 24.0.).

2.3 | Immunohistochemistry

For parvalbumin staining, brains of 6 *Gdnf*$^{wt/wt}$ and 6 *Gdnf*$^{wt/hyper}$ male mice aged 10–12 weeks were dissected out and fixed in 4% PFA (Sigma-Aldrich) for 72 hr at 4°C, cryoprotected in 30% sucrose, and cut into 40μm coronal slices with a cryostat (CM3050; Leica). Every sixth slice of the dorsal hippocampus between −1.355 mm and −2.488 mm anteroposteriorly was selected for staining and the distance between slices was 200 μm. Slices were then prepared for staining as described in Bespalov et al., 2011 rinsed in PBS, pH 7.4 and dehydrated in a series of methanol (30%, 50% and 80% in PBS), treated in Dent's fixative (80% methanol and 20% DMSO),

rinsed in TBSTD (TBS, 0.1% Tween and 5% DMSO), pH 7.4, and then blocked in BSA-TBSTD (5% BSA and 0.4% sheep serum in TBSTD) for 3 hr at room temperature. The slices were incubated in primary antibodies in BSA-TBSTD for 72 hr at 4°C using rabbit anti-parvalbumin (1:400, polyclonal, SYSY 195002). After washing in TBSTD three times, samples were placed overnight at 4°C with specific secondary antibodies (Alexa Fluor 568 goat anti–rabbit, 1:400; Invitrogen). Slices were then rinsed in TBSTD, incubated for one minute in Hoechst 33,342 (1:1,000; Invitrogen) and mounted on Superfrost Plus slides with ProLong Gold antifade reagent (Invitrogen) under coverslips. Parvalbumin positive hippocampal interneurons were imaged using a 4×/0.10 objective on an Olympus BX61 fluorescence microscope. Cell counts were performed with genotype blind to the experimenter in areas corresponding to the pyramidal layer of dorsal CA1, CA3 and the dentate gyrus of the hippocampal formation and in overlying cortical areas. Cell density was calculated as number of cells per mm^2 using ImageJ software using the selector method (Everall et al., 1997). Statistical analyses were performed in Graphpad Prism 7 (GraphPad Software).

For Nissl body staining, brains of 6 $Gdnf^{wt/wt}$ and 7 $Gdnf^{wt/hyper}$ male mice were cryosectioned to a thickness of 30μm every six sections and stored in cyropreservant buffer containing 30% ethylene glycol (Fisher) and 20% glycerol (Acros Organics) in phosphate buffer at −20°C until analysis. Sections were mounted and stained for Nissl bodies as described in Paul et al. (2008). Briefly, 5–7 sections beginning from the dorsal hippocampus were mounted on Superfrost Plus slides and allowed to dry overnight. Sections were then demyelinated, rehydrated, stained in warm cresyl-violet acetate, destained, dehydrated, cleared in xylene and mounted with permanent mounting media.

Stained sections were imaged using a Pannoramic 250 FLASH II slide scanner (3DHISTECH) at 20× magnification and analysed using the CaseViewer application. Ratios of hippocampal CA1 to dentate gyrus thickness were measured to assess potential hippocampal shrinkage, as described in Bittolo et al. (2016). Total thickness and thickness of layers 2/3 and 5/6 of overlying cortex were also measured. Cell density of hippocampal and cortical areas were calculated by counting the number of Nissl-stained cells in retrosplenial and posterior parietal cortex and in underlying dorsal hippocampal regions CA1, CA3 and dentate gyrus.

2.4 | In vitro electrophysiology

400 μm thick coronal hippocampal slices were prepared from 2 to 3 week-old male $Gdnf^{wt/wt}$ and $Gdnf^{wt/hyper}$ mice for electrophysiological recordings, $N = 7$ per genotype per procedure and 1–2 slices were used from each mouse. Mice were decapitated under general anaesthesia by placing 20 μl halothane (Sigma-Aldrich) onto a paper towel in a 500 ml covered plastic beaker and checking for signs of respiratory depression (<60 inhalations per minute) and testing for lack of paw withdrawal reflex, at which point brains were rapidly removed, dissected and cut with a vibratome in ice-cold standard solution containing (in mM): NaCl, 124; KCl, 3; CaCl, 2; NaHCO3, 26; NaH_2PO_4, 1.25; $MgSO_4$, 1.3; D-Glucose, 15 (Sigma-Aldrich) ; and equilibrated with 95% O_2/5% CO_2 to yield a pH of 7.4. The slices were allowed to recover for at least 1h at room temperature before being transferred into recording chamber. All recordings were carried out at 32°C in submerged configuration in standard solution.

Blind whole-cell patch-clamp recordings of IPSCs were made from CA1 pyramidal neurons using an Axopatch 200B amplifier (Axon Instruments). Internal solution for glass microelectrodes (5–7 MΩ) contained (in mM): $CsMeSO_4$, 130; HEPES, 10; NaCl, 8; EGTA, 0,5; QX314, 5; Mg-ATP, 4; Na-GTP, 0.3; 280 mOsm, pH adjusted to the final value of 7.2 with KOH (Sigma-Aldrich). Recordings were made in voltage-clamp mode at a holding potential of −70mV. Series resistance was monitored throughout the recordings and cells were rejected if values changed by more than 25% or exceeded 30 MΩ. Glutamate receptor antagonists D-AP5 (40 μM) and CNQX (10 μM) were added to the bathing solution to isolate GABAA receptor-mediated currents and record spontaneous inhibitory postsynaptic currents (sIPSCs). The voltage-dependent Na-channel dependent blocker tetrodotoxin (TTX, 1 μM) was added in combination with D-AP5 and NBQX to record action-potential-independent miniature spontaneous postsynaptic currents (mIPSCs). All drugs were from Tocris. IPSC frequency was measured from 200 s periods of continuous recordings. MiniAnalysis 6.0.3 (Synaptosoft Inc.) was used for analysis of IPSC data. sIPSCs and mIPSCs were detected using a peak detection algorithm of the software measuring peak amplitude, 10%–90% rise time and the time to decay (fraction of peak to find decay time was 37%). Undetected events and false positives were corrected by visual inspection. Threshold values were set at 2× the root mean square (2RMS) of baseline noise amplitude. Data were analysed blind as genotyping was performed post-hoc. Statistical analyses were performed in Graphpad Prism 7 (GraphPad Software) apart from the Kolmogorov–Smirnov tests performed online at http://www.physics.csbsju.edu/stats/KS-test.html (College of Saint Benedict and St John's University, MN, USA).

Field potential recordings of long-term potentiation (LTP) utilized the same procedure of sectioning brain slices as above. Slices were cut, stored and perfused as above and recordings were made in the same chamber using the same amplifier. Schaffer collateral afferents were stimulated with a bipolar stimulating electrode to elicit field excitatory

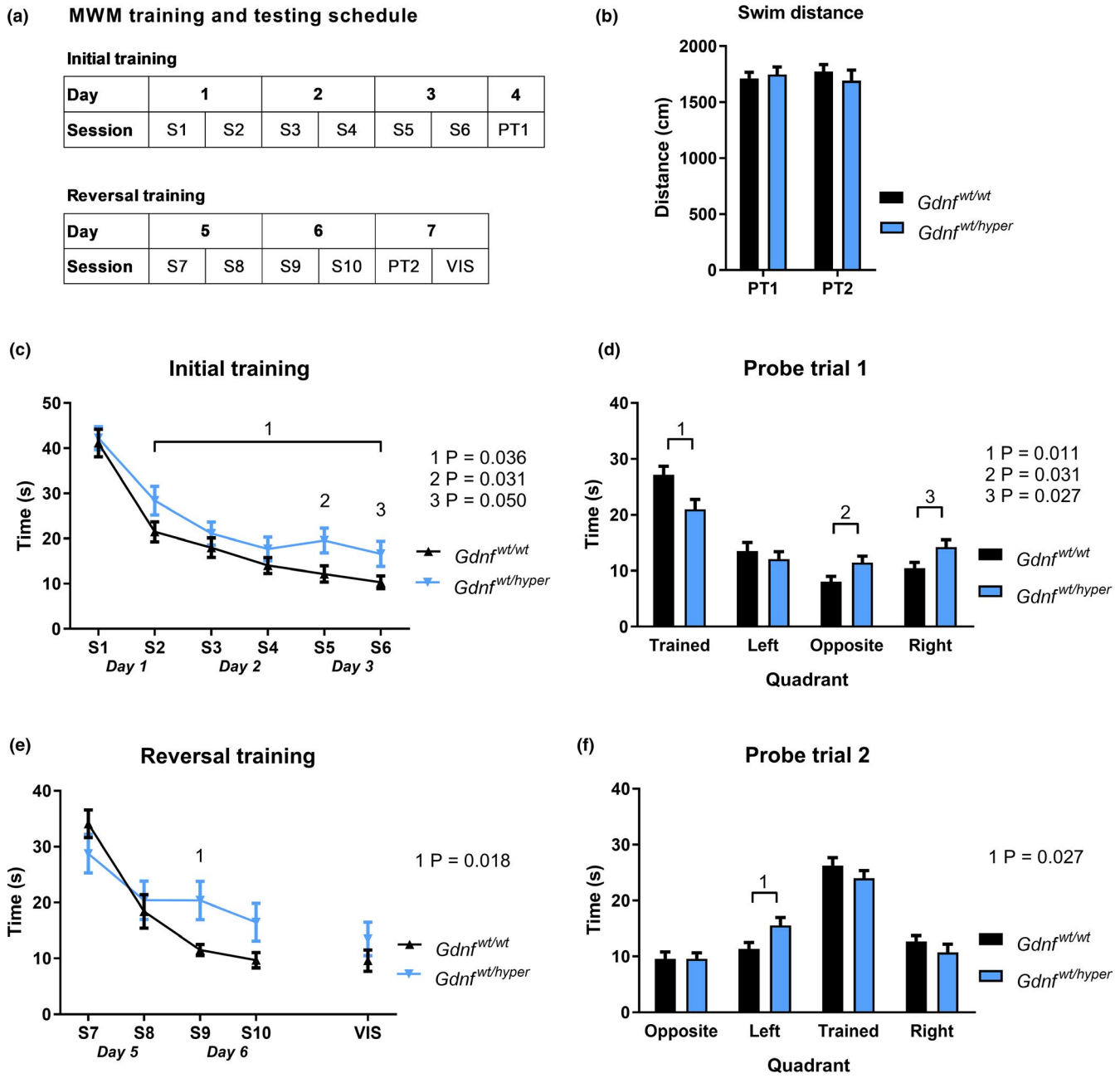

FIGURE 1 Morris water maze performance is impaired in $Gdnf^{wt/hyper}$ mice. All chart values are mean ± *SEM*. $Gdnf^{wt/wt}N = 22$, $Gdnf^{wt/hyper}N = 22$. 1A Training schedule for $Gdnf^{wt/wt}$ and $Gdnf^{wt/hyper}$ mice in the Morris water maze. S = session. PT = probe trial; two are performed on day 4 and two on day 7. VIS = average time to locate platform three times when it is visible and not submerged to see if escape latency is a factor. 1B Total swim distance in probe trials 1 and 2 as an indicator of motor activity. 1C Initial training of three sessions twice per day, 5 hr apart, 3 days in total. Statistical tests performed: 1 = two-way ANOVA, repeated measures; 2,3 = *t* test; 1D First probe trial; platform is removed and average time spent searching in each quadrant is recorded. Statistics: *t* test; $Gdnf^{wt/wt}N = 22$, $Gdnf^{wt/hyper}N = 21$. 1E Reversal training; platform is removed to the opposite quadrant and retraining takes places over 2 days. VIS = time spent swimming to platform that is made visible to see if escape latency is a factor. A *t* test was performed for *p*-values marked 1 and 2. 1F Second probe trial. Statistics: *t* test; $Gdnf^{wt/wt}N = 22$, $Gdnf^{wt/hyper}N = 21$

post-synaptic potentials (fEPSPs) in the stratum radiatum of hippocampal area CA1. Recordings were made using glass microelectrodes at a resistance of ~4 MΩ and filled with 150 mM NaCl. Baseline stimulation frequency was 0.05 Hz, pulse duration was 0.1 ms. LTP was induced by theta burst stimulation consisting of 10× 100 Hz bursts at an interval of 5 Hz. The LTP program (Anderson & Collingridge, 2001, University of Bristol, UK) was used for acquisition of fEPSP slope data. Data were normalized to the 20-min baseline prior to tetanic stimulation and the amount of LTP was assessed as the average increase in potentiation from 55 to 60 m after induction relative to baseline using a student's *t* test.

2.5 | Seizure threshold in vivo

Pentylenetetrazole (PTZ; Sigma-Aldrich) was administered intraperitoneally (i.p.) to a cohort of mature adult male mice aged 12–20 weeks comprised of 11 $Gdnf^{wt/hyper}$ and 13 $Gdnf^{wt/wt}$ wild-type littermate controls at an initial starting dose of 30 mg/kg and with additional top-up doses of 15 mg/kg at 5 m intervals until stage 5 seizure had been reached as scored via a modified Racine scale of seizure ratings (see Figure 4a). Seizures were video recorded using a standard webcam at 30fps and saved for analysis and verification. Mice were matched for body composition (mean weight = 34.54 g, *SD* = 5.14, min. = 27 g, max. = 45 g) as mice noted to be obese, weighing > 45 g had shorter latency to seizure in pilot experiments (data available on request). Statistical analyses were performed in Graphpad Prism 7 (GraphPad Software).

3 | RESULTS

3.1 | Deficits in memory performance in the Morris water maze

The Morris water maze is a well-established measure of memory performance in rodents. The first session requires the experimental animal to swim and locate a submerged platform hidden from view and to then locate it in subsequent sessions as a measure of dorsal hippocampal memory performance. In the initial search session $Gdnf^{wt/wt}$ *and* $Gdnf^{wt/hyper}$ mice demonstrate almost identical mean search times (see Figure 1c: $Gdnf^{wt/wt}$ $N = 22$, mean search time = 41.13s, *SEM* = 3.05; $Gdnf^{wt/hyper}$ $N = 22$, mean search time = 42.23s, *SEM* = 2.52; t=−0.279, $df = 42$, $p = .782$) indicating that there are no differences in the initial search strategy. However, a significantly impaired overall learning strategy in sessions S2–S6 was observed as a main effect between genotypes (Figure 1c: two-way ANOVA, repeated measures; $Gdnf^{wt/wt}$ $N = 22$, $Gdnf^{wt/hyper}$ $N = 22$; $F = 4.7$, $df = 2$, $p = .036$), with sessions 5 and 6 significantly impaired (*t*-test; $Gdnf^{wt/wt}$ $N = 22$, $Gdnf^{wt/hyper}$ $N = 22$; S5 $t = -2.233$, $df = 42$, $p = .031$; S6 $t = -2.018$, $df = 42$, $p = .050$). After three days of training in platform location, on the fourth day a probe trial session with no platform present is performed and the time spent in each quadrant of the swimming area is recorded. Upon probe trial training on day 4 after initial training completion, $Gdnf^{wt/hyper}$ mice spent significantly less time in the trained quadrant and significantly more time in the opposite and right quadrants, indicating impaired search performance (Figure 1d: *t* test; $Gdnf^{wt/wt}$ $N = 22$, $Gdnf^{wt/hyper}$ $N = 21$; Trained Quadrant $t = 2.666$, $df = 41$, $p = .011$; Opposite Quadrant $t = -2.236$, $df = 41$, $p = .031$; Right Quadrant $t = -2.295$, $df = 41$, $p = .027$). Reversal training is then performed with the platform in a different location for two days, on days 5 and 6. During reversal training, $Gdnf^{wt/hyper}$ again displayed a trend towards impaired learning overall (Figure 1e) that was however not statistically significant (two-way ANOVA, repeated measures; $Gdnf^{wt/wt}$ $N = 22$, $Gdnf^{wt/hyper}$ $N = 22$; $F = 2.774$, $df = 2$, $p = .103$), although session 9 was significantly impaired (*t* test; S9 $t = -2.461$, $df = 42$, $p = .018$). Upon testing with the reversal training probe trial with the platform removed, $Gdnf^{wt/hyper}$ again displayed an impaired search strategy and spent significantly more time in the left quadrant compared with wild-type mice (Figure 1f: *t* test; $Gdnf^{wt/wt}$ $N = 22$, $Gdnf^{wt/hyper}$ $N = 21$; Left Quadrant $t = -2.228$, $df = 41$, $p = .027$). No significant differences were found between $Gdnf^{wt/wt}$ and $Gdnf^{wt/hyper}$ in total swim distance in either probe trial 1 or 2 (Figure 1b), indicating no gross differences in motor activity. Therefore, $Gdnf^{wt/hyper}$ mice display significant impairment in memory compared to wild-type littermates and search performance across several measures in the MWM. These are not attributable to any increase in motor activity and suggest impaired memory function.

3.2 | Increased PV+ interneurons in dorsal hippocampus and in somatosensory and parietal cortex

Animals expressing GDNF binding receptor GFRα1 only in RET-positive cells display defective distribution of PV+ interneurons in the cortex (Canty et al., 2009). In order to assess parvalbumin-expressing interneuron density

FIGURE 2 Cortex and hippocampus show an increase in parvalbumin-positive interneurons. 2A Immunohistochemical fluorescent staining for the calcium-binding protein parvalbumin in $Gdnf^{wt/wt}$ and $Gdnf^{wt/hyper}$ mouse brain dorsal hippocampal coronal sections with rabbit anti-parvalbumin conjugated to Alex 568 goat anti-rabbit, magnified 4×, insets magnified a further 2×. 2B-2F Stereoscopic cell counts of parvalbumin-positive interneurons (PV+) in cortex and hippocampus. S1 trunk and posterior parietal are combined into a single region in 2C. Stastistical test are *t*-tests where $Gdnf^{wt/wt}N = 12$, $Gdnf^{wt/hyper}N = 14$. Chart values are mean ± *SEM*. 2G Nissl body staining of $Gdnf^{wt/wt}$ and $Gdnf^{wt/hyper}$ mouse brain dorsal hippocampal coronal sections. a = cortical thickness, b = cortical layers 2/3, c = cortical layers 5 + 6; d = CA1 and DG to the granule cell layer boundary of the DG upper blade, e = CA1, all layers from stratum oriens to stratum lacunosum moleculare. 2H Cortical thickness measurements of the entire cortex from layer 1 to the white matter tract below layer 6, and for layers 2/3 and 5 + 6 combined. All chart values are mean ± *SEM*. 2I CA1:dentate gyrus (DG) ratio. CA1 is measured perpendicularly from outer layer of the stratum oriens; DG is measured from the border of CA1 to the granule cell layer of the DG upper blade. 2J-2L Cell density measurements per millimetre in discrete cortical and hippocampal regions. All chart values are mean ± *SEM*. $Gdnf^{wt/wt}N = 6$, $Gdnf^{wt/hyper}N = 7$ for Nissl stains

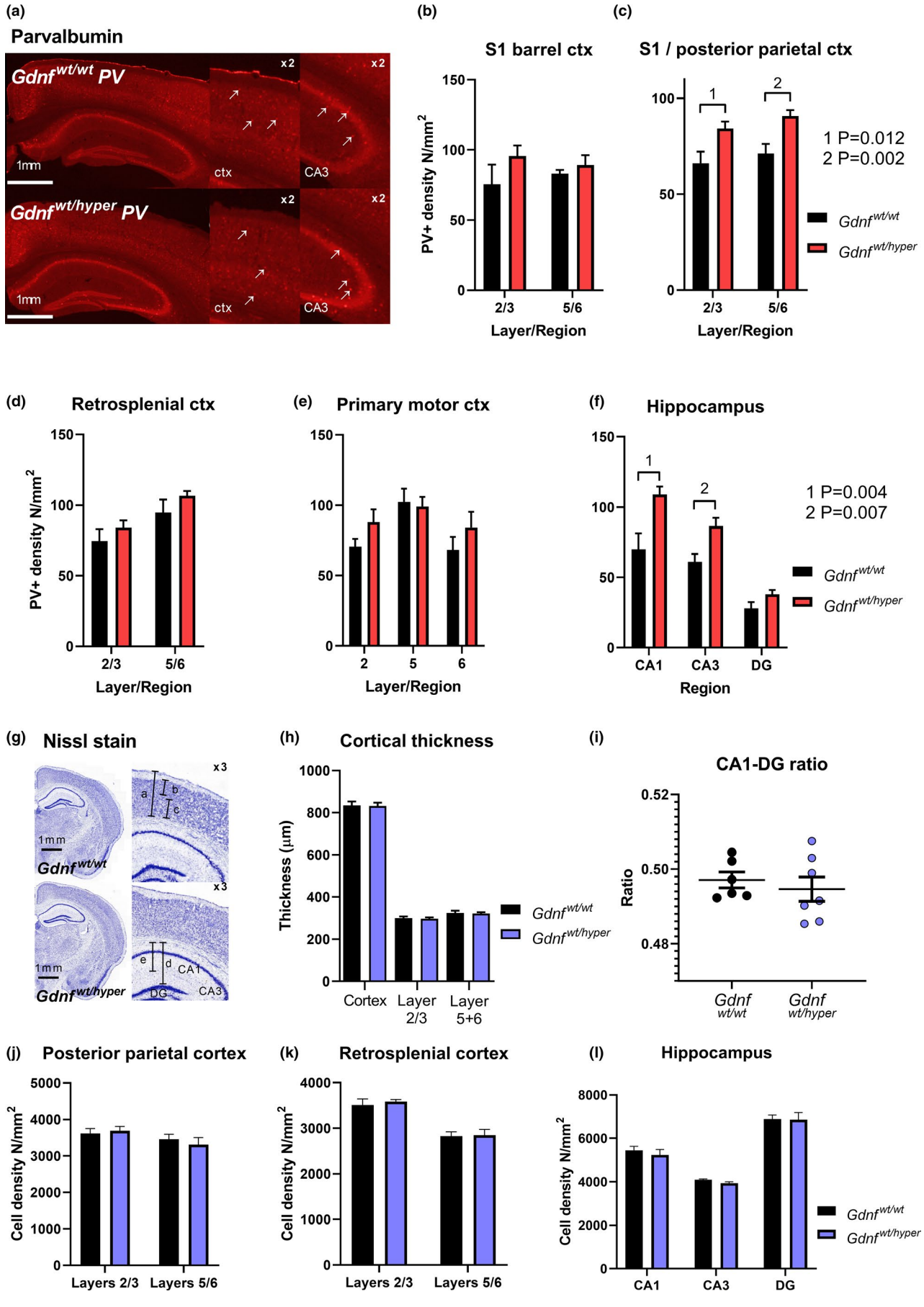

immunohistochemical staining for the calcium-binding protein parvalbumin was performed (see Figure 2a for representative sections). Cell density counts revealed that the number of parvalbumin-positive (PV+) interneurons per millimetre squared is significantly increased in *Gdnf*$^{wt/hyper}$ versus wild-type littermates in primary somatosensory (S1, trunk division) and posterior parietal cortex as shown in Figure 2c in layers 2/3 (*Gdnf*$^{wt/wt}$ $N = 12$, *Gdnf*$^{wt/hyper}$ $N = 14$, $t = -2.71$, $df = 24$, $p = .012$) and in layers 5–6 (*Gdnf*$^{wt/wt}$ $N = 12$, *Gdnf*$^{wt/hyper}$ $N = 14$, $t = -3.39$, $df = 24$, $p = .002$;). No significant differences were seen in S1 barrel cortex (Figure 2b), nor in retrosplenial or primary motor cortex (M1), (Figure 2d,e). A significant increase in PV+ cell density was also seen in hippocampal areas CA1 (*Gdnf*$^{wt/wt}$ $N = 12$, *Gdnf*$^{wt/hyper}$ $N = 14$, $t = -3.22$, $df = 24$, $p = .004$) and in CA3 (*Gdnf*$^{wt/wt}$ $N = 12$, *Gdnf*$^{wt/hyper}$ $N = 14$, $t = -3.10$, $df = 24$, $p = .007$) but not in dentate gyrus, as shown in Figure 2f.

An apparent increase in PV+ cell density could be due to a decrease in cortical or hippocampal thickness, or due to an overall increase in cell density. To analyse those option cell density and cortical and hippocampal thickness were measured using Nissl staining. Representative sections show no gross differences in morphology (Figure 1g). Nissl body staining of coronal brain sections at the same level of the dorsal hippocampus as those used for staining of parvalbumin revealed no significant differences in cortical thickness (Figure 2h) or in the thickness of layer 2/3 or layers 5 + 6. There was no difference in the CA1:DG size ratio between *Gdnf*$^{wt/hyper}$ and wild-type littermates (Figure 2i), as measured perpendicularly from the stratum oriens of CA1, through stratum radiatum to the granule cell layer of the dentate gyrus at the centre of the upper blade. Cell density measurements in posterior parietal cortex, retrosplenial cortex, and in hippocampus (Figure 2j–l) revealed no significant differences. No gross differences in morphology were observed (Figure 2g).

3.3 | Increased GABAergic tone in hippocampus in vitro

To gain further insight into how an increase in PV+ cell number influences hippocampal function we next performed electrophysiological measurements in the hippocampus. Alterations in memory performance in vivo as observed in the MWM could be reflected in altered capacity for memory formation, so a standard long-term potentiation (LTP) protocol was measured in CA1 in 400μm acute hippocampal slices via theta burst stimulation (Figure 3a,b). However no significant differences between *Gdnf*$^{wt/hyper}$ and wild-type littermates were observed when comparing the means of the last 5 min of recording, 55–60 min post-tetanus, normalized to baseline (*Gdnf*$^{wt/wt}$ $N = 4$, Gdnf$^{wt/hyper}$ $N = 6$; $t = 1{,}398$, $df = 8$, $p = .199$). Increased PV+ cell density is however suggestive of altered GABAergic signalling that may impact memory performance on the MWM. Therefore, GABAergic tone was monitored in vitro via spontaneous and miniature post-synaptic currents. These were recorded in acute hippocampal slices, as above, using a blind patch configuration. Measurement revealed a typical peak amplitude profile (Figure 3c,d) whereby mIPSCs are normally distributed and sIPSCs have a positive skew; the latter necessitating a non-parametric Kolmogorov–Smirnov test for statistical analysis of amplitude. sIPSC amplitude was significantly increased in *Gdnf*$^{wt/hyper}$ as shown by a rightward shift in the cumulative amplitude curve (Figure 3g: Kolmogorov-Smirnov; $D = 0.128$, $p = .0006$). This was accompanied by a significant increase in sIPSC mean frequency in *Gdnf*$^{wt/hyper}$ versus wild-type littermates (Figure 3e: *Gdnf*$^{wt/wt}$ $N = 6$, *Gdnf*$^{wt/hyper}$ $N = 7$; $t = -2.22$, $df = 14$, $p = .043$) and a significant leftward shift in the cumulative frequency curve for *Gdnf*$^{wt/hyper}$ (Figure 3f: Kolmogorov–Smirnov; $D = 0.35$, $p = .001$). No significant differences were seen in mIPSC frequency or amplitude (Figure 3h–j), suggesting that an increased number of PV+ cells firing action potentials – perhaps as a network – is the predominant effect over basal, quantal GABA release onto pyramidal cells in CA1.

3.4 | Increased seizure threshold in vivo

To further corroborate the increase in GABAergic tone seen in vitro, in vivo seizure threshold was measured with intraperitoneal application of pentylenetetrazole. A significant increase in latency to stage 5 seizures in *Gdnf*$^{wt/hyper}$ versus wild-type littermates was observed (Figure 4b: *Gdnf*$^{wt/wt}$ $N = 13$, *Gdnf*$^{wt/hyper}$ $N = 11$, $t = 2.14$, $df = 22$, $p = .044$)

FIGURE 3 Increased GABAergic tone in vitro. 3A-B Long-term potentiation in acute 400 μm dorsal hippocampal sections from *Gdnf*$^{wt/wt}$ and *Gdnf*$^{wt/hyper}$ mice. Values normalized to baseline and mean ± *SEM* is given for each data point. LTP induction occurs at time 20 m using theta burst stimulation. *Gdnf*$^{wt/wt}$ $N = 4$, Gdnf$^{wt/hyper}$ $N = 6$ animals and analysed via *t* test, $p > .05$. 3C-D amplitude histograms given for spontaneous and miniature inhibitory post-synaptic currents (s/mIPSCs) in *Gdnf*$^{wt/wt}$ and *Gdnf*$^{wt/hyper}$ mice with values binned for amplitude on the *x*-axis. 3E sIPSC mean frequency; chart values are mean ± *SEM*. Statistical test: *t* test. 3F Cumulative plot of sIPSC inter-event interval in milliseconds, statistical test: Kolmogorov–Smirnov. 3G Cumulative plot of sIPSC amplitude in Picoamperes on a base-10 logarithmic scale. Statistical test: Kolmogorov–Smirnov. 3H mIPSC mean frequency; chart values are mean ± *SEM*. 3I Cumulative plot of mIPSC inter-event interval in milliseconds. 3J Cumulative plot of sIPSC amplitude in Picoamperes on a base-10 logarithmic scale. *Gdnf*$^{wt/wt}$ $N = 6$, *Gdnf*$^{wt/hyper}$ $N = 7$ animals for patch-clamp recordings

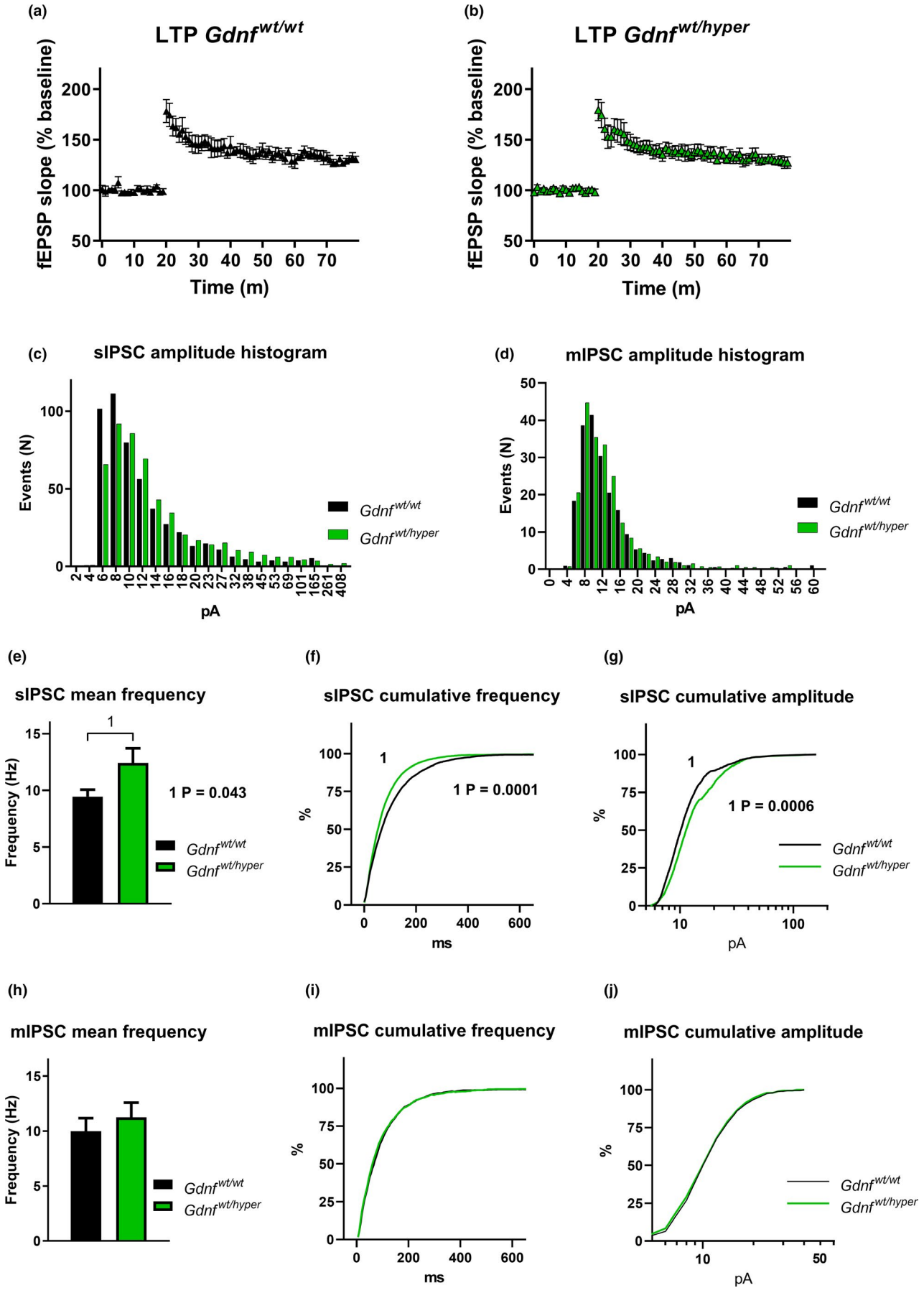

(a)

Racine scale of seizure classification

Stage	Characterisation
1	Decrease in motor activity until comes to rest; time at which abdomen makes contact with cage.
2	Twitches. First whole body head to tail hiccups.
3	Time to first fall, with recovery. Fully developed minimal seizures with head and forelimb clonus.
4	Falls and remains prone. Forelimbs parallel to body axis and stiff.
5	Wild running and jumping (WRJ). Major seizure resulting in fall and clonus of all limbs usually leading to death.

(b) **Latency to stage 5 seizure**

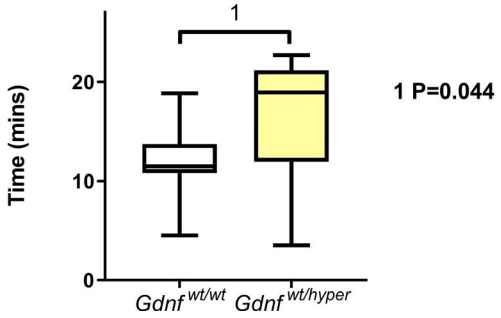

FIGURE 4 Increased seizure threshold in vivo. 4A Racine scale of seizure classification modified for mouse behaviour. 4B Horizontal line denotes mean latency to stage 5 seizure in $Gdnf^{wt/wt}$ and $Gdnf^{wt/hyper}$ mice. Boxplots represent 25th and 75th percentiles, bars represent range of minimum and maximum values. Statistical test: *t* test, $Gdnf^{wt/wt}$ $N = 13$, $Gdnf^{wt/hyper}$ $N = 11$ animals

according to a modified Racine scale of behavioural seizure classification (Figure 4a). It therefore appears that altered GABAergic signalling manifests as some resistance to seizures in $Gdnf^{wt/hyper}$ mice and supports the notion that it is inhibitory signalling that is increased; to the extent that epileptic seizures are delayed, in vivo.

4 | DISCUSSION

Previous work on the effects of GDNF signalling on interneuron development studied either embryonic development in genetic knockout mice or utilized GFRα1 "cis-only" mice where perinatally-induced lethality is overcome by only expressing the GDNF receptor GFRa1 in RET-expressing cells. This transgenic model of GFRα1 knockout revealed PV+ "holes" in various areas in the cortex and reduced threshold to seizures (Canty et al., 2009). Conversely, here we have studied $Gdnf^{wt/hyper}$ mice that over-express GDNF protein only in natively expressing cells. These mice survive and gain weight normally (Kumar et al., 2015) and display a normal behavioural repertoire (Mätlik et al., 2018), thus enabling analysis of the postnatal effects of a constitutive increase in GDNF expression without altering the pattern of expression. We observed significant impaired memory performance in young adult mice in the Morris water maze during initial training and testing and somewhat impaired memory performance during reversal training and testing. The lesser effects in reversal training as compared to initial training may be due to confounding factors upon memory function due to repeat training and testing over multiple days increasing the signal-to-noise ratio for detection.

The memory component of the platform location task is largely dependent upon dorsal hippocampal function (Moser et al., 1995). Given this evidence of reduced dorsal hippocampal function we then measured classical long-term potentiation (LTP) in stratum radiatum of CA1 via theta-burst stimulation yet observed no significant impairments in excitability analogous to memory formation. We did however observe increased inhibitory tone in the hippocampus that was paralleled by an increased number of PV+ interneurons in the hippocampus and in several cortical areas. This increase in PV+ cell number was not attributable to gross changes in cell density, cortical layer thickness, or hippocampal size as ascertained by Nissl staining. As increased GABAergic activity in the hippocampus is known to be protective against chemically-induced seizures (Martin et al., 1995; Yoo et al., 2006), we next found that $Gdnf^{wt/hyper}$ mice are indeed protected from PTZ-induced seizures. However, why does a persistent, twofold increase in endogenous GDNF levels impair memory retrieval in young adult mice?

In hippocampal slice preparations in vitro both the frequency and amplitude of sIPSCs (spontaneous inhibitory post-synaptic currents) were increased in CA1 pyramidal cells of $Gdnf^{wt/hyper}$ mice compared to wild-type littermates.These results are consistent with a larger population of interneurons firing simultaneously. Additional changes in interneuronal intrinsic excitability and/or restructuring of inter-interneuron connectivity may mediate the observed increase in frequency. This increase in GABAergic network activity is postulated to have an effect on memory because GABA (Klausberger et al., 2005) and, more specifically, parvalbumin-positive interneurons (Ognjanovski et al., 2017) are important regulators of hippocampal oscillations (Ylinen et al., 1995) during memory consolidation immediately following learning and in the consolidation that occurs during sleep. As mIPSCs (miniature inhibitory post-synaptic currents) showed no increase in frequency or amplitude this suggests that the observed increase in GABAergic tone is not due to increased quantal release of GABA, nor to increased GABAA receptor number (Nusser et al., 1997), but rather due to increased inhibitory network activity.

Although GDNF has also been shown to regulate excitatory synapse formation in the hippocampus (Irala

et al., 2016) we did not observe hyperexcitability in *Gdnf*$^{wt/hyper}$ mice in response to pentylenetetrazole challenge; on the contrary, they were protected. While Canty et al. (2009) did not observe changes in hippocampal PV+ neuron number in GFRα1 "cis-only" mice, we did observe an increase in PV+ cell number in the CA1 and CA3 pyramidal layers in *Gdnf*$^{wt/hyper}$ mice, suggesting that RET-independent GDNF signalling may be a factor in hippocampal PV+ neuron development and positioning. The observed increase in PV+ cells in the cortex in *Gdnf*$^{wt/hyper}$ mice complements the previous observation in GFRα1 cis-only mice (Canty et al., 2009) and suggests that GDNF is the likely ligand for GFRα1 in driving cortical PV+ neuron development.

A recent study suggested that PV+-dependent long-term memory consolidation has a critical time window of 12–14 hr post-training (Karunakaran et al., 2018). This supports our observations as impairments in recall become apparent only after consolidation: during training on day 3, in the probe trial on day 4, and in reversal training on day 5. The same study also showed that memory consolidation is dependent upon dopamine (DA) D1/D5 receptors. So far it is known that complete ablation of GDNF does not alter DA levels or DAergic cell survival (Kopra et al., 2015) but instead modifies dopamine transporter (DAT) function in the striatum (Kopra et al., 2017). *Gdnf* heterozygous knockout mice do however exhibit a learning and memory deficit (Gerlai et al., 2001), again without any changes in striatal DA or the DA metabolite 3,4-dihydroxyphenylacetic acid (DOPAC) levels. We have, however, previously reported in these *Gdnf*$^{wt/hyper}$ mice a 25% increase in striatal DA concentration and a 35%–40% increase in striatal DOPAC along with greatly enhanced dopamine transporter (DAT) function (Kumar et al., 2015). Although dopamine release in the hippocampus is correlated with episodic and spatial memory learning (Kempadoo et al., 2016) it is possible that increased dopamine turnover may occur in the hippocampus of *Gdnf*$^{wt/hyper}$ mice and be a factor in impaired memory consolidation.

PV+ cell number is known to directly affect seizure threshold and PV+ interneurons are particularly sensitive to epileptic insult in both mice (Bouilleret et al., 2000; Kuruba et al., 2011) and in humans (Maglóczky & Freund, 2005). Pharmacological ablation of PV+ interneurons in mice results in the development of spontaneous seizures (Drexel et al., 2017) and optogenetic stimulation of PV+ interneurons abolishes seizures in mice (Krook-Magnuson et al., 2013). However, ectopic GDNF overexpression in and of itself supresses seizures in rodent models (Boscia et al., 2009; Kanter-Schlifke et al., 2007, 2009; Waldau et al., 2010; Yoo et al., 2006) and, although in those experiments GDNF expression generally far exceeds endogenous GDNF expression levels by two or more orders of magnitude, we cannot exclude that the around twofold increase in endogenous GDNF expression in *Gdnf*$^{wt/hyper}$ mice supresses seizure threshold directly and independently of increased PV+ cell number. Decreased seizure threshold has been reported in a GFRα1R cis-only knockout mouse model in response to pentylenetetrazole (PTZ) challenge (Canty et al., 2009). We observed an increased seizure threshold in *Gdnf*$^{wt/hyper}$ mice that appears to compliment this previous work. Experiments with inducible *Gdnf* ^{hyper} or conditional knockout *Gdnf* ^{hyper} mice in the future would shed further light upon whether this is an acute or developmental effect of GDNF expression in native cells. Activation of PV+ neurons has been shown to attenuate temporal lobe epilepsy (TLA) (Wang et al., 2018) and loss of PV+ neurons to precede juvenile myoclonic epilepsy in a Brd2 mouse model (McCarthy et al., 2020). Altered PV+ function is also seen in schizophrenia and bipolar disorder (Ferguson & Gao, 2018; Toker et al., 2018), Fragile X syndrome (Goel et al., 2018), Tourette syndrome and autism (Rapanelli et al., 2017). Therefore, there may be therapeutic benefits to understanding the relationship between interneuronal function and GDNF.

ACKNOWLEDGEMENTS

This study was supported by Instrumentarium Foundation grant to PM, the Academy of Finland (1308265, 266820 to CR, 297727 to JOA), the Sigrid Juselius Foundation (CR, JOA), the University of Helsinki Doctoral Programme Brain and Mind (DRG), Faculty of Medicine at the University of Helsinki, Helsinki Institute of Life Science Fellow grant (JOA), European Research Council (ERC) nr 724922 (JOA) and by Alzheimerfonden (JOA). VV was supported by Jane and Aatos Erkko Foundation; Mouse Behavioural Phenotyping Facility was supported by Biocenter Finland and Helsinki Institute of Life Science. The authors also thank Prof Mart Saarma for his enormous support, for initiating the in vivo GDNF studies and providing funding from the Sigrid Juselius Foundation and the Academy of Finland.

CONFLICT OF INTEREST

The authors declare no conflicts of interest.

AUTHOR CONTRIBUTIONS

PM designed and performed all experiments and statistical analyses except for the Morris water maze and Nissl stain and wrote the manuscript. DRG performed Nissl stain and created related figures and text, performed related statistical analysis and edited some sections of the manuscript. TT provided facilities and reagents for the in vitro electrophysiology experiments. VV provided facilities and funding for the Morris water maze experiments. CV and NK performed the Morris water maze experiments. CR provided facilities, reagents and funding for immunohistochemistry and in vivo seizure experiments and aided with implementation of the latter and edited some sections of the manuscript. JOA

proposed the study, supplied the transgenic mice, edited and co-wrote several sections of the paper, and provided funding.

PEER REVIEW

The peer review history for this article is available at https://publons.com/publon/10.1111/ejn.15126.

DATA AVAILABILITY STATEMENT

All supporting data and materials can be accessed at the corresponding author's host institution at University of Helsinki, HiLIFE Neuroscience Centre, Helsinki, Finland.

ORCID

Pepin Marshall https://orcid.org/0000-0002-3620-1889

REFERENCES

Anderson, W. W., & Collingridge, G. L. (2001). The LTP Program: a data acquisition program for on-line analysis of long-term potentiation and other synaptic events. *J Neurosci Methods*, *108*(1), 71–83. https://doi.org/10.1016/s0165-0270(01)00374-0

Bespalov, M. M., Sidorova, Y. A., Tumova, S., Ahonen-Bishopp, A., Magalhães, A. C., Kulesskiy, E., Paveliev, M., Rivera, C., Rauvala, H., Saarma, M., Magalhaes, A. C., Kulesskiy, E., Paveliev, M., Rivera, C., Rauvala, H., & Saarma, M. (2011). Heparan sulfate proteoglycan syndecan-3 is a novel receptor for GDNF, neurturin, and artemin. *Journal of Cell Biology*, *192*, 153–169.

Bittolo, T., Raminelli, C. A., Deiana, C., Baj, G., Vaghi, V., Ferrazzo, S., Bernareggi, A., & Tongiorgi, E. (2016). Pharmacological treatment with mirtazapine rescues cortical atrophy and respiratory deficits in MeCP2 null mice. *Scientific Reports*, *6*, 19796.

Boscia, F., Esposito, C. L., Di Crisci, A., de Franciscis, V., Annunziato, L., & Cerchia, L. (2009). GDNF selectively induces microglial activation and neuronal survival in CA1/CA3 hippocampal regions exposed to NMDA insult through Ret/ERK signalling. *PLoS One*, *4*, e6486. https://doi.org/10.1371/journal.pone.0006486

Bouilleret, V., Loup, F., Kiener, T., Marescaux, C., & Fritschy, J. M. (2000). Early loss of interneurons and delayed subunit-specific changes in GABA(A)-receptor expression in a mouse model of mesial temporal lobe epilepsy. *Hippocampus*, *10*, 305–324. https://doi.org/10.1002/1098-1063(2000)10:3<305:AID-HIPO11>3.0.CO;2-I

Canty, A. J., Dietze, J., Harvey, M., Enomoto, H., Milbrandt, J., & Ibáñez, C. F. (2009). Regionalized loss of parvalbumin interneurons in the cerebral cortex of mice with deficits in GFRalpha1 signaling. *Journal of Neuroscience*, *29*, 10695–10705.

Chen, Y., & Bradley, A. (2000). A new positive/negative selectable marker, puΔtk, for use in embryonic stem cells. *Genesis*, *28*, 31–35. https://doi.org/10.1002/1526-968X(200009)28:1<31:AID-GENE40>3.0.CO;2-K

Cobb, S. R., Buhl, E. H., Halasy, K., Paulsen, O., & Somogyi, P. (1995). Synchronization of neuronal activity in hippocampus by individual GABAergic interneurons. *Nature*, *378*, 75–78. https://doi.org/10.1038/378075a0

Donato, F., Rompani, S. B., & Caroni, P. (2013). Parvalbumin-expressing basket-cell network plasticity induced by experience regulates adult learning. *Nature*, *504*, 272–276. https://doi.org/10.1038/nature12866

Drexel, M., Romanov, R. A., Wood, J., Weger, S., Heilbronn, R., Wulff, P., Tasan, R. O., Harkany, T., & Sperk, G. (2017). Selective silencing of hippocampal parvalbumin interneurons induces development of recurrent spontaneous limbic seizures in mice. *Journal of Neuroscience*, *37*, 8166–8179.

Durbec, P., Marcos-Gutierrez, C. V., Kilkenny, C., Grigoriou, M., Wartiowaara, K., Suvanto, P., Smith, D., Ponder, B., Costantini, F., Saarma, M., Sariola, H., & Pachnis, V. (1996). GDNF signalling through the Ret receptor tyrosine kinase. *Nature*, *381*, 789–793. https://doi.org/10.1038/381789a0

Enomoto, H., Araki, T., Jackman, A., Heuckeroth, R. O., Snider, W. D., Johnson, E. M., & Milbrandt, J. (1998). GFR alpha 1-deficient mice have deficits in the enteric nervous system and kidneys. *Neuron*, *21*, 317–324.

Everall, I. P., DeTeresa, R., Terry, R., & Masliah, E. (1997). Comparison of two quantitative methods for the evaluation of neuronal number in the frontal cortex in Alzheimer disease. *Journal of Neuropathology and Experimental Neurology*, *56*, 1202–1206.

Ferguson, B. R., & Gao, W.-J. (2018). PV interneurons: Critical regulators of E/I balance for prefrontal cortex-dependent behavior and psychiatric disorders. *Frontiers in Neural Circuits*, *12*, 1–13. https://doi.org/10.3389/fncir.2018.00037

Fukuda, T., & Kosaka, T. (2000a). Gap junctions linking the dendritic network of GABAergic interneurons in the hippocampus. *Journal of Neuroscience*, *20*, 1519–1528. https://doi.org/10.1523/JNEUROSCI.20-04-01519.2000

Fukuda, T., & Kosaka, T. (2000b). The dual network of GABAergic interneurons linked by both chemical and electrical synapses: A possible infrastructure of the cerebral cortex. *Neuroscience Research*, *38*, 123–130. https://doi.org/10.1016/S0168-0102(00)00163-2

Galanopoulou, A. S. (2010). Mutations affecting GABAergic signaling in seizures and epilepsy. *Pflügers Archiv: European Journal of Physiology*, *460*, 505–523.

Gerlai, R., McNamara, A., Choi-Lundberg, D. L., Armanini, M., Ross, J., Powell-Braxton, L., & Phillips, H. S. (2001). Impaired water maze learning performance without altered dopaminergic function in mice heterozygous for the GDNF mutation. *European Journal of Neuroscience*, *14*, 1153–1163.

Goel, A., Cantu, D. A., Guilfoyle, J., Chaudhari, G. R., Newadkar, A., Todisco, B., de Alba, D., Kourdougli, N., Schmitt, L. M., Pedapati, E., Erickson, C. A., & Portera-Cailliau, C. (2018). Impaired perceptual learning in a mouse model of Fragile X syndrome is mediated by parvalbumin neuron dysfunction and is reversible. *Nature Neuroscience*, *21*, 1404–1411. https://doi.org/10.1038/s41593-018-0231-0

Humpel, C., Hoffer, B., Strömberg, I., Bektesh, S., Collins, F., & Olson, L. (1994). Neurons of the hippocampal formation express glial cell line-derived neurotrophic factor messenger RNA in response to kainate-induced excitation. *Neuroscience*, *59*, 791–795. https://doi.org/10.1016/0306-4522(94)90284-4

Ibáñez, C. F., & Andressoo, J.-O.-O. (2015). Biology of GDNF and its receptors – Relevance for disorders of the central nervous system. *Neurobiology of Diseases*, *97*, 80–89.

Irala, D., Bonafina, A., Fontanet, P. A., Alsina, F. C., Paratcha, G., & Ledda, F. (2016). GDNF/GFRα1 complex promotes development of hippocampal dendritic arbors and spines via NCAM. *Development*, 4224–4235.

Jing, S. Q., Wen, D. Z., Yu, Y. B., Holst, P. L., Luo, Y., Fang, M., Tamir, R., Antonio, L., Hu, Z., Cupples, R., Louis, J. C., Hu, S., Altrock, B. W., & Fox, G. M. (1996). GDNF-induced activation of the Ret

protein tyrosine kinase is mediated by GDNFR-alpha, a novel receptor for GDNF. *Cell*, *85*, 1113–1124.

Kanter-Schlifke, I., Fjord-Larsen, L., Kusk, P., Angehagen, M., Wahlberg, L., & Kokaia, M. (2009). GDNF released from encapsulated cells suppresses seizure activity in the epileptic hippocampus. *Experimental Neurology*, *216*, 413–419.

Kanter-Schlifke, I., Georgievska, B., Kirik, D., & Kokaia, M. (2007). Seizure suppression by GDNF gene therapy in animal models of epilepsy. *Molecular Therapy*, *15*, 1106–1113.

Karunakaran, S., Chowdhury, A., Donato, F., Quairiaux, C., Michel, C. M., & Caroni, P. (2018). Author correction: PV plasticity sustained through D1/5 dopamine signaling required for long-term memory consolidation. *Nature Neuroscience*, *21*, 1290. https://doi.org/10.1038/s41593-018-0179-0

Kawaguchi, Y., Katsumaru, H., Kosaka, T., Heizmann, C. W., & Hama, K. (1987). Fast spiking cells in rat hippocampus (CA1 region) contain the calcium-binding protein parvalbumin. *Brain Research*, *416*, 369–374.

Kempadoo, K. A., Mosharov, E. V., Choi, S. J., Sulzer, D., & Kandel, E. R. (2016). Dopamine release from the locus coeruleus to the dorsal hippocampus promotes spatial learning and memory. *Proceedings of the National Academy of Sciences of the United States of America*, *113*, 14835–14840.

Klausberger, T., Marton, L. F., O'Neill, J., Huck, J. H. J., Dalezios, Y., Fuentealba, P., Suen, W. Y., Papp, E., Kaneko, T., Watanabe, M., Csicsvari, J., & Somogyi, P. (2005). Complementary roles of cholecystokinin- and parvalbumin-expressing GABAergic neurons in hippocampal network oscillations. *Journal of Neuroscience*, *25*, 9782–9793.

Kopra, J. J., Panhelainen, A., af Bjerkén, S., Porokuokka, L. L., Varendi, K., Olfat, S., Montonen, H., Piepponen, T. P., Saarma, M., & Andressoo, J.-O. (2017). Dampened amphetamine-stimulated behavior and altered dopamine transporter function in the absence of brain GDNF. *Journal of Neuroscience*, *37*, 1581–1590.

Kopra, J., Vilenius, C., Grealish, S., Harma, M.-A., Varendi, K., Lindholm, J., Castren, E., Voikar, V., Bjorklund, A., Piepponen, T. P., Saarma, M., & Andressoo, J.-O. (2015). GDNF is not required for catecholaminergic neuron survival in vivo. *Nature Neuroscience*, *18*, 319–322.

Krook-Magnuson, E., Armstrong, C., Oijala, M., & Soltesz, I. (2013). On-demand optogenetic control of spontaneous seizures in temporal lobe epilepsy. *Nature Communications*, *4*, 1376–1378.

Kumar, A., Kopra, J., Varendi, K., Porokuokka, L. L., Panhelainen, A., Kuure, S., Marshall, P., Karalija, N., Härma, M. A., Vilenius, C., Lilleväli, K., Tekko, T., Mijatovic, J., Pulkkinen, N., Jakobson, M., Jakobson, M., Ola, R., Palm, E., Lindahl, M., … Andressoo, J. O. (2015a). GDNF overexpression from the native locus reveals its role in the nigrostriatal dopaminergic system function. *PLoS Genetics*, *11*, 1–24. https://doi.org/10.1371/journal.pgen.1005710

Kuruba, R., Hattiangady, B., Parihar, V. K., Shuai, B., & Shetty, A. K. (2011). Differential susceptibility of interneurons expressing neuropeptide Y or parvalbumin in the aged hippocampus to acute seizure activity. *PLoS One*, *6*, e24493. https://doi.org/10.1371/journal.pone.0024493

Lin, L. F., Doherty, D. H., Lile, J. D., Bektesh, S., & Collins, F. (1993). GDNF: A glial cell line-derived neurotrophic factor for midbrain dopaminergic neurons. *Science*, *260*, 1130–1132. https://doi.org/10.1126/science.8493557

Maglóczky, Z., & Freund, T. F. (2005). Impaired and repaired inhibitory circuits in the epileptic human hippocampus. *Trends in Neurosciences*, *28*, 334–340.

Marín, O. (2012). Interneuron dysfunction in psychiatric disorders. *Nature Reviews Neuroscience*, *13*, 107–120.

Markram, H., Toledo-Rodriguez, M., Wang, Y., Gupta, A., Silberberg, G., & Wu, C. (2004). Interneurons of the neocortical inhibitory system. *Nature Reviews Neuroscience*, *5*, 793–807.

Martin, D., Miller, G., Rosendahl, M., & Russell, D. A. (1995). Potent inhibitory effects of glial derived neurotrophic factor against kainic acid mediated seizures in the rat. *Brain Research*, *683*, 172–178.

Mätlik, K., Võikar, V., Vilenius, C., Kulesskaya, N., & Andressoo, J. (2018). Two-fold elevation of endogenous GDNF levels in mice improves motor coordination without causing side-effects. *Scientific Reports*, *8*, 11861.

McCarthy, E., Shakil, F., Saint Ange, P., Morris Cameron, E., Miller, J., Pathak, S., Greenberg, D. A., Velíšková, J., & Velíšek, L. (2020). Developmental decrease in parvalbumin-positive neurons precedes increase in flurothyl-induced seizure susceptibility in the Brd2+/− mouse model of juvenile myoclonic epilepsy. *Epilepsia*, *61*, 892–902.

Mikuni, N., Babb, T. L., Chakravarty, D. N., & Christi, W. (1999). Time course of transient expression of GDNF protein in rat granule cells of the bilateral dentate gyri after unilateral intrahippocampal kainic acid injection. *Neuroscience Letters*, *262*, 215–218. https://doi.org/10.1016/S0304-3940(99)00074-9

Moore, M. W., Klein, R. D., Fariñas, I., Sauer, H., Armanini, M., Phillips, H., Reichardt, L. F., Ryan, A. M., Carver-Moore, K., & Rosenthal, A. (1996). Renal and neuronal abnormalities in mice lacking GDNF. *Nature*, *382*, 76–79. https://doi.org/10.1038/382076a0

Moser, M. B., Moser, E. I., Forrest, E., Andersen, P., & Morris, R. G. (1995). Spatial learning with a minislab in the dorsal hippocampus. *Proceedings of the National Academy of Sciences of the United States of America*, *92*, 9697–9701.

Nusser, Z., Cull-Candy, S., & Farrant, M. (1997). Differences in synaptic GABA(A) receptor number underlie variation in GABA mini amplitude. *Neuron*, *19*, 697–709. https://doi.org/10.1016/S0896-6273(00)80382-7

Ognjanovski, N., Schaeffer, S., Wu, J., Mofakham, S., Maruyama, D., Zochowski, M., & Aton, S. J. (2017). Parvalbumin-expressing interneurons coordinate hippocampal network dynamics required for memory consolidation. *Nature Communications*, *8*, 15039.

Olsen, R. W., & Avoli, M. (1997). GABA and epileptogenesis. *Epilepsia*, *38*, 399–407. https://doi.org/10.1111/j.1528-1157.1997.tb01728.x

Paratcha, G., Ledda, F., & Ibáñez, C. F. (2003). The neural cell adhesion molecule NCAM is an alternative signaling receptor for GDNF family ligands. *Cell*, *113*, 867–879. https://doi.org/10.1016/S0092-8674(03)00435-5

Paul, C. A., Beltz, B., & Berger-Sweeney, J. (2008). The Nissl stain: A stain for cell bodies in brain sections. *Cold Spring Harbor Protocols*, *2008*(10), pdb.prot4805. https://doi.org/10.1101/pdb.prot4805

Pichel, J. G., Shen, L., Sheng, H. Z., Granholm, A. C., Drago, J., Grinberg, A., Lee, E. J., Huang, S. P., Saarma, M., Hoffer, B. J., Sariola, H., & Westphal, H. (1996). Defects in enteric innervation and kidney development in mice lacking GDNF. *Nature*, *382*, 73–76. https://doi.org/10.1038/382073a0

Pozas, E., & Ibáñez, C. F. (2005). GDNF and GFRalpha1 promote differentiation and tangential migration of cortical GABAergic neurons. *Neuron*, *45*, 701–713.

Rapanelli, M., Frick, L. R., & Pittenger, C. (2017). The role of interneurons in autism and Tourette Syndrome. *Trends in Neurosciences*, *40*, 397–407.

Reeben, M., Laurikainen, A., Hiltunen, J. O., Castren, E., & Saarma, M. (1998). The messenger RNAs for both glial cell line-derived neurotrophic factor receptors, c-ret and GDNFR alpha, are induced in the rat brain in response to kainate-induced excitation. *Neuroscience*, *83*, 151–159.

Sánchez, M. P., Silos-Santiago, I., Frisén, J., He, B., Lira, S. A., & Barbacid, M. (1996). Renal agenesis and the absence of enteric neurons in mice lacking GDNF. *Nature*, *382*, 70–73. https://doi.org/10.1038/382070a0

Sarabi, A., Hoffer, B. J., Olson, L., & Morales, M. (2000). GFR alpha-1 is expressed in parvalbumin GABAergic neurons in the hippocampus. *Brain Research*, *877*, 262–270.

Schmidt-Kastner, R., Tomac, A., Hoffer, B., Bektesh, S., Rosenzweig, B., & Olson, L. (1994). Glial cell-line derived neurotrophic factor (GDNF) mRNA upregulation in striatum and cortical areas after pilocarpine-induced status epilepticus in rats. *Brain Research. Molecular Brain Research*, *26*, 325–330.

Toker, L., Mancarci, B. O., Tripathy, S., & Pavlidis, P. (2018). Transcriptomic evidence for alterations in astrocytes and parvalbumin interneurons in subjects with bipolar disorder and schizophrenia. *Biological Psychiatry*, *84*(11), 787–796. https://doi.org/10.1016/j.biopsych.2018.07.010

Treanor, J. J. S., Goodman, L., deSauvage, F., Stone, D. M., Poulsen, K. T., Beck, C. D., Gray, C., Armanini, M. P., Pollock, R. A., Hefti, F., Phillips, H. S., Goddard, A., Moore, M. W., BujBello, A., Davies, A. M., Asai, N., Takahashi, M., Vandlen, R., Henderson, C. E., & Rosenthal, A. (1996). Characterization of a multicomponent receptor for GDNF. *Nature*, *382*, 80–83. https://doi.org/10.1038/382080a0

Trupp, M., Arenas, E., Fainzilber, M., Nilsson, A. S., Sieber, B. A., Grigoriou, M., Kilkenny, C., Salazar-Grueso, E., Pachnis, V., Arumae, U., Sariola, H., Saarma, M., Ibanez, C. F., SalazarGrueso, E., Pachnis, V., Arumae, U., Sariola, H., Saarma, M., & Ibanez, C. F. (1996). Functional receptor for GDNF encoded by the c-ret proto-oncogene. *Nature*, *381*, 785–789. https://doi.org/10.1038/381785a0

Võikar, V., Rossi, J., Rauvala, H., & Airaksinen, M. S. (2004). Impaired behavioural flexibility and memory in mice lacking GDNF family receptor α2. *European Journal of Neuroscience*, *20*, 308–312.

Waldau, B., Hattiangady, B., Kuruba, R., & Shetty, A. K. (2010). Medial ganglionic eminence-derived neural stem cell grafts ease spontaneous seizures and restore GDNF expression in a rat model of chronic temporal lobe epilepsy. *Stem Cells*, *28*, 1153–1164. https://doi.org/10.1002/stem.446

Wang, Y., Liang, J., Chen, L., Shen, Y., Zhao, J., Xu, C., Wu, X., Cheng, H., Ying, X., Guo, Y., Wang, S., Zhou, Y., Wang, Y., & Chen, Z. (2018). Pharmaco-genetic therapeutics targeting parvalbumin neurons attenuate temporal lobe epilepsy. *Neurobiology of Diseases*, *117*, 149–160.

Ylinen, A., Bragin, A., Nádasdy, Z., Jandó, G., Szabó, I., Sik, A., & Buzsáki, G. (1995). Sharp wave-associated high-frequency oscillation (200 Hz) in the intact hippocampus: Network and intracellular mechanisms. *Journal of Neuroscience*, *15*, 30–46. https://doi.org/10.1523/JNEUROSCI.15-01-00030.1995

Yoo, Y.-M., Lee, C.-J., Lee, U., & Kim, Y.-J. (2006a). Neuroprotection of adenoviral-vector-mediated GDNF expression against kainic-acid-induced excitotoxicity in the rat hippocampus. *Experimental Neurology*, *200*, 407–417. https://doi.org/10.1016/j.expneurol.2006.02.132

How to cite this article: Marshall P, Garton DR, Taira T, et al. Elevated expression of endogenous glial cell line-derived neurotrophic factor impairs spatial memory performance and raises inhibitory tone in the hippocampus. *Eur J Neurosci*. 2021;53:2469–2482. https://doi.org/10.1111/ejn.15126